AIMS Materials Science, 13(2): 240–257.
DOI: 10.3934/matersci.2026014
Received: 28 November 2025
Revised: 13 February 2026
Accepted: 04 March 2026
Published: 12 March 2026

https://www.aimspress.com/journal/Materials

Research article

Simulation of the effect of atomic ratio Ti/Al and C/N on the properties of TiAlCN film by molecular dynamics method

Duc Luan Nguyen and Duc Cuong Pham*

HaUI Institute of Technology, Hanoi University of Industry, Hanoi, Vietnam

* **Correspondence:** Email: phamcuong@haui.edu.vn; Tel: +84-094-489-1969.

Abstract: TiAlCN coatings are increasingly widely applied in practice. Mathematical models of the formation and development of these coatings provide a foundation for researchers to predict and control their physical, chemical, and mechanical properties. In this paper, we present an atomic-scale molecular dynamics model for the growth of TiAlCN coatings, in which the deposition conditions are designed to represent typical cathodic arcs' evaporation parameters. By describing the deposition process of Ti, Al, C, and N atoms on the Fe substrate's surface, we evaluate the influence of Ti/Al and C/N atomic ratios on the hardness, friction coefficient, and surface roughness of TiAlCN coatings. These properties are critical for applications in mechanical fields, such as cutting tools and molds. The simulation results show that the maximum hardness of the TiAlCN coating is 31 GPa at a Ti/Al ratio of 7:3 and 36 GPa at a C/N ratio of 5:5. The minimum roughness is 3.83 Å at a Ti/Al ratio of 7:3 and 3.82 Å at a C/N ratio of 5:5. The lowest friction coefficient is 0.38 at a Ti/Al ratio of 7:3 and 0.25 at a C/N ratio of 5:5. These results are consistent with the experimental findings, confirming the reliability of the proposed theoretical model.

Keywords: TiAlCN thin films; atomic ratio; hardness; surface roughness; nanoindentation

1. Introduction

Transition metal nitride coatings, such as TiAlN and TiAlCN, have revolutionized surface engineering, enhancing the durability and performance of cutting tools, molds, and high-load components in industrial applications [1–3]. TiAlCN coatings, incorporating C and N into the TiAlN

matrix, stand out for their superior combination of high hardness, low friction, excellent wear resistance, and outstanding thermal stability [4–6]. These properties stem from the interplay of the inherent hardness of TiN, the oxidation resistance of AlN, and carbon phases resembling diamond-like carbon (DLC), which enhance the tribological performance [7–9]. These characteristics make TiAlCN coatings particularly suitable for high-speed machining of difficult-to-cut materials, such as titanium alloys and stainless steel, improving tools' life and operational efficiency [10,11].

The performance of TiAlCN coatings depends heavily on their chemical composition, particularly the Ti/Al and C/N atomic ratios, which determine phase composition, microstructure, and mechanical properties [12–14]. The Ti/Al ratio governs the balance between hard TiN phases and thermally stable AlN phases. A high Ti content promotes crystalline TiN structures, increasing hardness, while a high Al content enhances oxidation resistance through the formation of protective Al_2O_3 layers at high temperatures [15]. Similarly, the C/N ratio influences the incorporation of carbon into the nitride matrix, with high carbon content forming sp^2-hybridized phases that reduce friction but may decrease hardness if amorphous structures dominate [16]. Experimental studies report hardness values for TiAlCN coatings ranging from 28 to 44 GPa, friction coefficients as low as 0.2–0.3, and a surface roughness (Ra) below 2.5 nm under optimal conditions [17]. However, the mechanisms by which the Ti/Al and C/N ratios affect films' growth and properties remain complex, necessitating detailed atomic-level investigations [18,19].

Molecular dynamics (MD) reveals the impact of these ratios on phase composition, grain size, defect formation, and surface morphology. MD offers a cost-effective approach to systematically investigate compositional effects, guiding the optimization of TiAlCN coatings for high-speed machining and wear-resistant applications. By predicting hardness, roughness, and tribological performance, MD simulations provide a robust framework for designing tailored coatings with enhanced durability and low friction. This study uses MD simulation to investigate the effects of Ti/Al and C/N atomic ratios on the hardness and surface roughness of TiAlCN coatings on Fe substrates. By systematically varying these ratios, we aim to elucidate the atomic mechanisms governing the films' growth, including phase formation, defect development, and surface morphology. The results are expected to provide valuable insights for optimizing the composition of coatings to enhance mechanical and tribological performance, reducing reliance on experimental optimization, and advancing the development of high-performance coatings for industrial applications. This research bridges the gap between experimental and theoretical studies, offering detailed insights into how atomic-level compositional variations translate into macroscopic coating properties for applications in aerospace, automotive, and precision manufacturing. With MD simulations, the atomic ratio can be tested in multiple models instead of through experiments. This significantly saves material costs, fabrication time, and analysis effort, and provides an initial quantitative database to support the design of industrial-scale TiAlCN coatings.

This study focuses on simulating the formation of TiAlCN coatings on Fe substrates with different Ti/Al ratios (1:9, 3:7, 5:5, 7:3, and 9:1) and C/N ratios (1:9, 3:7, 5:5, 7:3, and 9:1). It then determines the effects of these atomic ratios on surface hardness and roughness, and proposes the optimal ranges of atomic ratios to achieve coatings with a hardness of >30 GPa and a roughness of <5 Å. The expected results will provide a solid theoretical foundation for selecting the chemical composition and technological conditions to fabricate high-quality TiAlCN coatings with significantly reduced research and development costs.

Due to the absence of direct experimental validation in this study, the simulation results are systematically compared and discussed with experimental findings reported in the literature on TiAlCN and related TiAlN/TiCN coatings, in order to assess the reliability and physical relevance of the proposed model [2,9,12,19].

2. Materials and methods

2.1. Fundamental principles

MD is a critical tool for studying physical systems at the atomic and molecular levels over time. This method uses Newton's classical equations of motion to simulate the movement of atoms and molecules, based on interatomic forces calculated through potential functions. In this study, the modified embedded atom method (MEAM), Tersoff, and Vashishta potential functions are applied to simulate the formation of TiAlCN coatings on Fe substrates, aiming to analyze the material's mechanical and structural properties. The MEAM is a semiempirical many-body potential, and is an improvement over the embedded atom method (EAM). The MEAM accounts for interactions between an atom and multiple neighboring atoms, beyond pairwise interactions, enabling accurate simulation of properties such as elastic constants and defect formation energies in metals. This is particularly useful for studying TiAlCN coatings, which have complex structures involving multiple elements [20]. Tersoff potential is designed to describe systems with covalent bonding, such as semiconductors (silicon, germanium), carbon (diamond, graphene), and ceramics (SiC, AlN). It is a many-body potential where the bond energy between two atoms depends not only on their distance but also on the surrounding environment, including the number and angles of neighboring bonds. The bond order parameter of Tersoff potential allows a flexible description of variations in bond strength, making it suitable for simulating materials like TiAlCN [21]. Vashishta potential, developed by Priya Vashishta's group, incorporates Coulombic, charge-dipole, van der Waals, and angular energy interactions, based on the Stillinger–Weber potential. This potential is designed to simulate complex systems, particularly ceramics and multielement compounds like TiAlCN, where many-body interactions and bond angles play a crucial role in determining the structural and mechanical properties [22].

A hybrid interatomic potential scheme was used to account for the coexistence of metallic, covalent, and mixed bonding in the TiAlCN system, following the established MD practices implemented in the large-scale atomic/molecular massively parallel simulator (LAMMPS) [20–23].

2.2. Configuration of the simulation box

Although the plasma generated during cathodic arc evaporation is not explicitly simulated, the MD model focuses on the atomic-scale deposition and growth of the TiAlCN film by assigning incident energies, fluxes, substrate temperatures, and bias voltages consistent with cathodic arc conditions.

The LAMMPS is an atomic simulation tool that uses prebuilt commands to perform classical MD simulations, enabling the modeling of both solid-state materials and soft matter. It is a software platform capable of handling large-scale systems by leveraging parallel computing. The simulation box in this study consists of three main regions: The active region, the thermostat region, and the fixed region, as illustrated in Figure 1. The active region is where atoms can move and interact directly under the influence of relevant forces, governed by the interaction potential function. The thermostat region

controls the temperature of the entire system, with the Langevin thermostat algorithm [23] applied to maintain stable temperatures. The fixed region serves as a rigid support to ensure the simulation's stability. Periodic boundary conditions are applied in the *x* and *y* directions within the plane of the TiAlCN coating, whereas nonperiodic boundary conditions are established in the *z* direction to more accurately reflect the deposition process. To ensure the system's stability, the deposition process simulation is conducted under NVT (N (number of particles): the number of atoms/particles is kept constant; V (volume): the volume of the simulation box remains fixed; T (temperature): the temperature is controlled and maintained at a stable value) conditions with varying temperature levels.

The simulation box has dimensions of 100 × 60 × 50 Å, comprising a substrate layer of 20 Å, a fixed layer of 15 Å, a thermal layer of 5 Å, and an active layer of 30 Å. We ensured that the thickness of the fixed layer and the thermal layer were equal to the thickness of the substrate, as shown in Figure 1. The system's equations of motion are numerically integrated with a time step of dt = 1 fs [24].

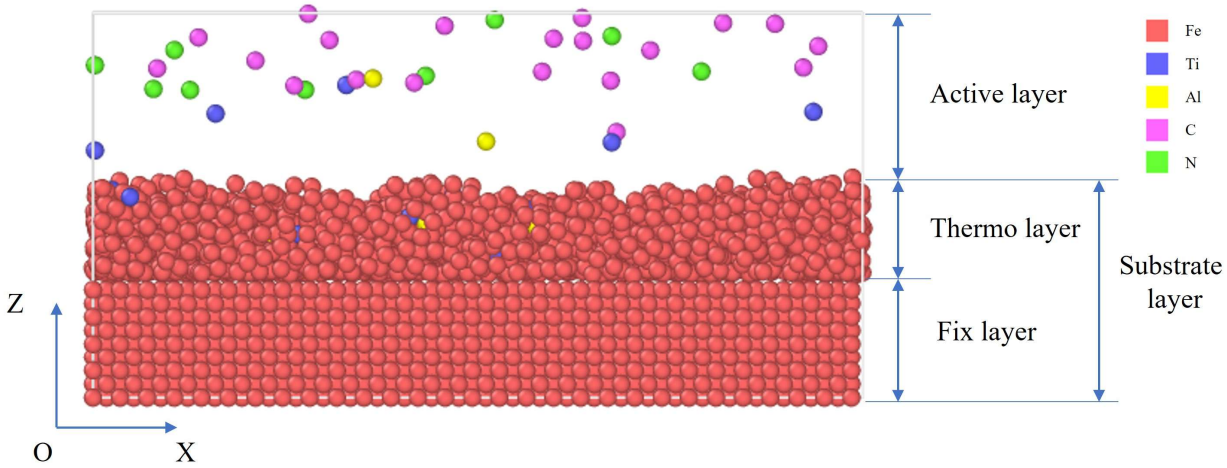

Figure 1. Simulation model illustrating the influence of atomic ratios on the properties of the TiAlCN film.

2.3. Simulation parameters for investigating the influence of the Ti/Al atomic ratio on the TiAlCN film's growth

We assumed the ideal gas equation of state as Eq 1:

$$n = \frac{PV}{RT} \tag{1}$$

where n represents the theoretical molar amount of gas, P is the pressure, V is the gas volume at temperature T, R = 8.314 J·mol^{-1}·K^{-1}, is the universal gas constant, and T is the temperature in degrees Kelvin. In the simulation of film deposition, the typical pressure is set to $P = 5 \times 10^{-2}$ Pa. The gas volume V in the ideal gas equation was varied as the input value (60, 180, 300, 420, and 540 standard cubic centimeters per minute (SCCM)). In the MD simulation, the gas flow rate (in SCCM) is implemented indirectly by adjusting the number of atoms inserted per unit of time (the deposition flux). Thus, the variation in V reflects different gas flow conditions, while the practical implementation in the simulation is achieved through controlled atom insertion rather than continuous gas dynamics. The numbers of Ti and Al atoms listed in Tables 1 and 2 are intentionally different, as they were calculated

according to the prescribed Ti:Al atomic ratios, rather than being assumed to be equal. Similarly, the numbers of C and N atoms were determined from the relative gas ratios of C_2H_2 and N_2 introduced into the vacuum chamber. In this study, the Ti:Al and C:N ratios were systematically varied as 1:9, 3:7, 5:5, 7:3, and 9:1. This approach enables the simulated coating compositions to realistically represent a wide range of TiAlCN coatings with different elemental ratios. On this basis, the number of Ti, Al, C, and N atoms is calculated as shown in Tables 1 and 2. Other simulation parameters are kept constant: The arc current is 80 A, the substrate temperature is 673 K, and the bias voltage is –100 V [25–27]. Within the framework of MD, the effects of the arc current and the substrate's polarization voltage are demonstrated indirectly by controlling the deposition flux and initial kinetic energy of the incoming materials, rather than by directly applying electrical parameters. Although the total number of atoms varies slightly between different simulation sets, the simulation box's size, the duration of deposition, and the analysis protocol were kept identical to ensure a meaningful comparison of relative trends.

Table 1. Simulation input parameters affecting the C/N atomic ratio of the TiAlCN coating.

No.	Ti velocity (Å/ps)	Al velocity (Å/ps)	C velocity (Å/ps)	N velocity (Å/ps)	Bias voltage (V)	Substrate temperature (K)	Quantity of C	Quantity of N	Quantity of Ti	Quantity of Al
1	11.22	14.21	1.43	2.54	–100	673	646	5815	4522	1938
2							1938	4522		
3							3230	3230		
4							4522	1938		
5							5815	646		

Table 2. Simulation input parameters affecting the Ti/Al atomic ratio of the TiAlCN coating.

No.	Ti velocity (Å/ps)	Al velocity (Å/ps)	C velocity (Å/ps)	N velocity (Å/ps)	Bias voltage (V)	Substrate temperature (K)	Quantity of C	Quantity of N	Quantity of Ti	Quantity of Al
1	11.22	14.21	1.43	2.54	–100	673	5815	4522	1938	646
2									1938	4522
3									3230	3230
4									4522	1938
5									5815	646

2.4. Simulation of some properties of the TiAlCN film

For all results examined for all samples obtained by the physical vapor deposition (PVD) method, the following steps were carried out before testing the composition, hardness, and friction coefficient.

During the deposition process, atoms with very high energy, when bonded together, generate local stresses on the coating's surface. Therefore, the system's energy was initially minimized by adjusting the atomic coordinates step by step until the sample reached a stable state, using the min_style algorithm. Next, the system was equilibrated under NVT conditions, allowing overlapping atoms in the system to relax, thus achieving an equilibrium state for the TiAlCN coating.

2.4.1. Simulation of the hardness of the TiAlCN film

In hardness simulations, the nanoindentation process is modeled by applying a virtual indenter (typically a Berkovich or spherical tip) onto the surface of the film. The main steps are shown in the flowchart below (Figure 2).

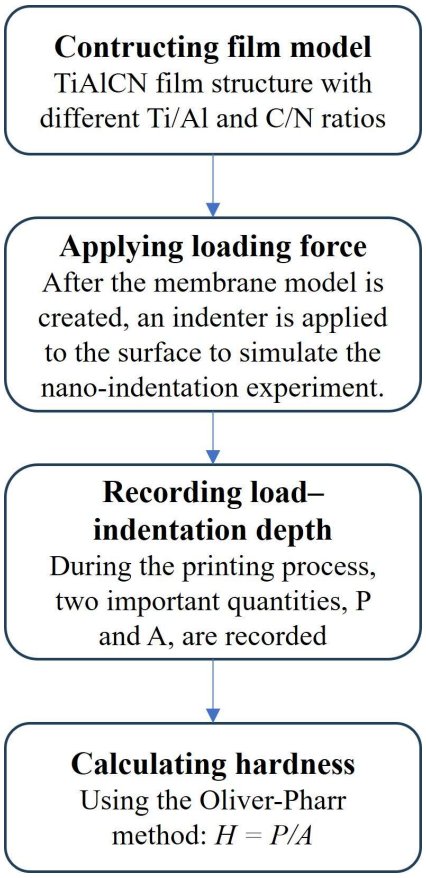

Figure 2. Flowchart of the hardness calculation process.

In these calculations, H is the hardness of the film (GPa), P is the applied normal load (Newtons), and A is the contact area between the indenter and the film. The applied load P is extracted from the computed force output in the LAMMPS simulation script. The contact area A in nanoindentation simulations is typically calculated according to the shape of the indenter (Eq 2):

$$A = \pi\delta(2R - \delta) \tag{2}$$

where R is the radius of the indenter's tip and δ is the indentation depth from the surface of the thin film. In the elastic region, the hardness is calculated using $H = P/A$. Its value remains stable with only minor fluctuations, reflecting the material's deformation response under different indenter impacts. The hardness was simulated using an indenter with a radius of R = 10 Å. The indentation depth can be selected according to $0.3 \leq R/h \leq 6.2$ [28].

P can be calculated using Eq 3 [25]:

$$P(r) = -K(r - R)^2 \tag{3}$$

where K = 10 eV/Å^3, is a constant defining the force, r is the distance from the atom to the center of the indenter, R is the radius of the indenter, and $P(r) = 0$ with $r > R$.

2.4.2. Simulation of the coefficient of friction of TiAlCN thin films

MD is an effective computational technique for simulating the coefficient of friction of materials, particularly thin films like TiAlCN, by reproducing atomic-scale interactions during sliding contact. MD is based on solving Newton's equations of motion for a system of atoms, using interatomic potential functions of Ti/Al (such as Tersoff or the MEAM) to describe the forces between atoms. In coefficient of friction simulations, a sliding contact model is established, typically simulating a sliding contact experiment. The main steps are shown in the flowchart in Figure 3.

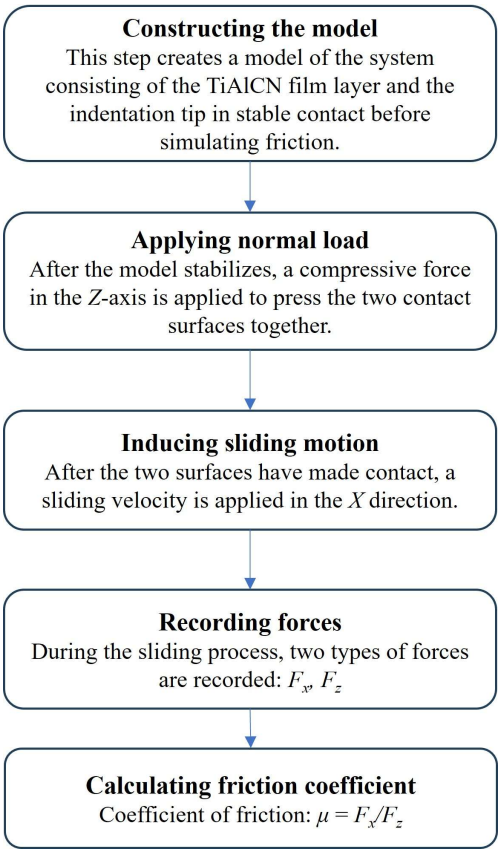

Figure 3. Flowchart of the coefficient of friction calculation process.

In Figure 3, μ is coefficient of frictions, Fz is the total force component in the vertical direction, and Fx is the total force component in the horizontal (Ox) direction. In this model, a virtual indenter is pressed into a surface and moves with a constant velocity. The indenter can have various sizes and shapes (such as spherical, hemispherical, prismatic, cylindrical, etc.). It remains in contact with the surface throughout the entire simulation process.

2.4.3. Simulation of the surface roughness of TiAlCN thin films

There are several methods for determining the surface roughness of thin films: atomic force microscopy (AFM), scanning electron microscopy (SEM), stylus profilometry, light scattering analysis, and MD simulation. The tool OVITO was used to visualize the simulation results, display the deposition process, and analyze surface morphology.

The surface roughness of the deposited films is expressed by the root mean square (RMS) of the roughness value (R_s), which is calculated as Eq 4 [29]:

$$R_s = \sqrt{\frac{\sum_{i=1}^{n}(Z_i - Z_{mean})^2}{n}} \tag{4}$$

where Z_i is the z-coordinate of the topmost atoms in each region, Z_{mean} is the average height of the Z-coordinates of the topmost atoms in each region, and n is the total number of atoms on the surface of the coating.

To ensure the reliability of the simulation's results, all systems were fully relaxed through energy minimization and equilibrated under NVT conditions prior to property evaluation. The interatomic potentials used in this work have been widely validated for Ti–Al–C–N systems. Furthermore, the simulated trends and absolute values of hardness, the friction coefficient, and surface roughness are consistent with the experimental results reported in the literature for TiAlCN coatings.

3. Results

3.1. Hardness

A virtual indenter with a radius of R = 15 Å was pressed into the film to a depth of 15 Å, and the resulting plot is shown in Figure 4. In the nanoindentation simulation, the spherical indenter is initially placed above the film surface and then gradually pressed into the coating. Therefore, the indentation depth shown in Figure 4 represents the actual penetration depth of the indenter in contact with the film.

For each composition, several independent nanoindentation simulations were carried out at different surface positions, and the reported hardness values represent the average, with the error estimated as the standard deviation.

From Figure 5, it can be observed that at high Ti/Al ratios (such as 9:1 or 7:3), the high Ti content promotes the formation of the cubic phase of TiAlCN, based on the TiN structure, which inherently possesses high hardness (25–32 GPa). The strong Ti–N and Ti–C bonds are the primary factors contributing to the superior hardness, with further enhancement attributed to the Hall–Petch effect (hardness increases as grain size decreases). In contrast, when the Al content is higher, the structure tends to shift toward a hexagonal AlN-based phase, resulting in a reduction in the overall hardness to approximately 22–24 GPa, as shown in Figure 5. This reduction in hardness can be attributed to the increasing fraction of AlN-based phases. Unlike cubic TiN and TiC, which exhibit high hardness caused by strong covalent–ionic bonding, AlN tends to form a hexagonal wurtzite structure with significantly lower intrinsic hardness.

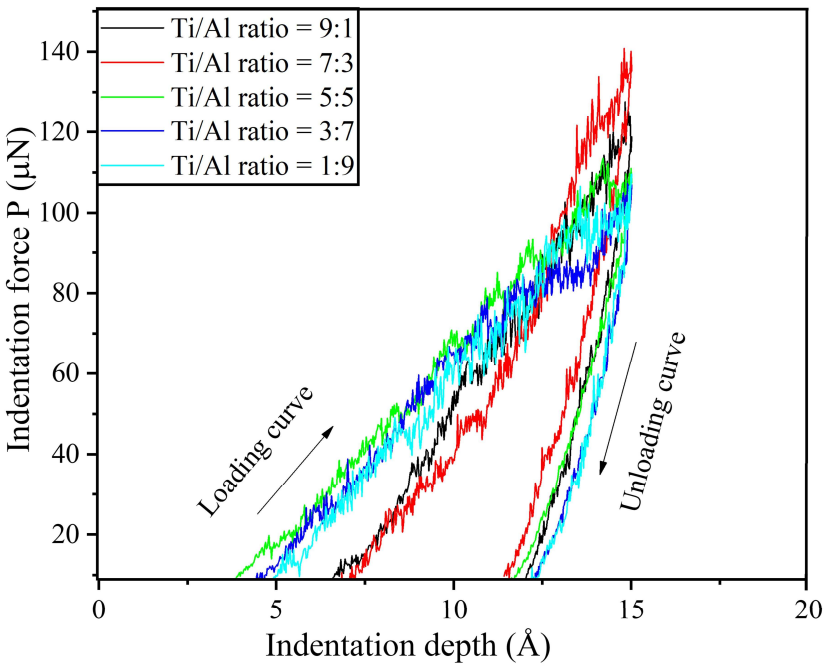

Figure 4. Graph showing the process of testing the effect of the Ti/Al atomic ratio on the hardness of the TiAlCN film.

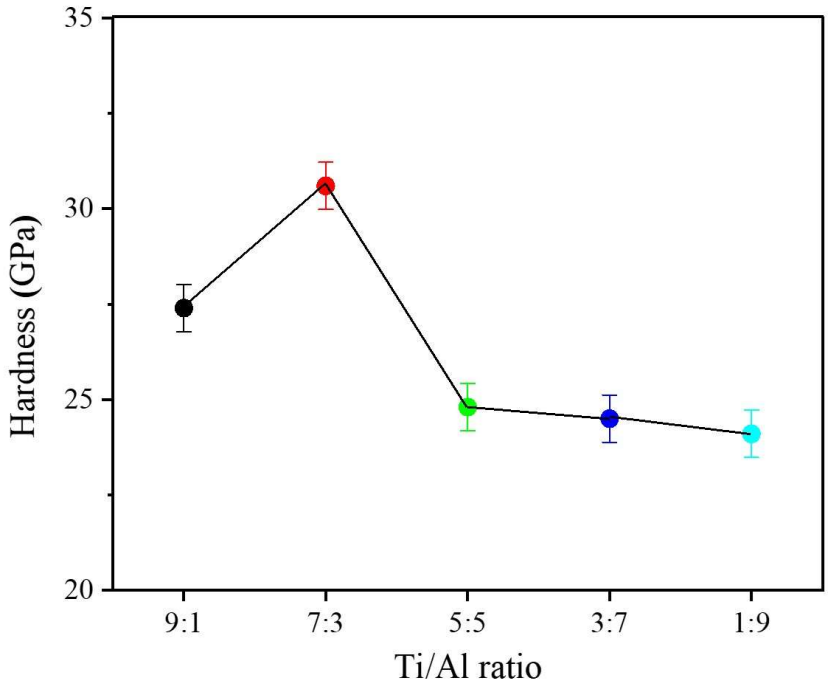

Figure 5. Graph illustrating the effect of the Ti/Al atomic ratio on the hardness of the TiAlCN film.

The indentation depth shown in Figure 6 represents the actual penetration depth of the indenter in contact with the film. Varying the C/N atomic ratio significantly alters the intrinsic structure of the TiAlCN coating. At high C/N ratios, excess carbon promotes the formation of C–C bonds and amorphous carbon-rich regions, which disrupt long-range order and reduce structural rigidity [9,12,19]. Conversely,

increasing the nitrogen content enhances Ti–N bonding, favoring the formation of more ordered TiN-based nanocrystalline domains [2,19]. At an intermediate C/N ratio (≈5:5), a mixed nanocomposite structure consisting of TiN/TiC nanocrystalline phases embedded in a carbon-containing amorphous matrix is formed, combining crystalline reinforcement with microstructural refinement [9,19].

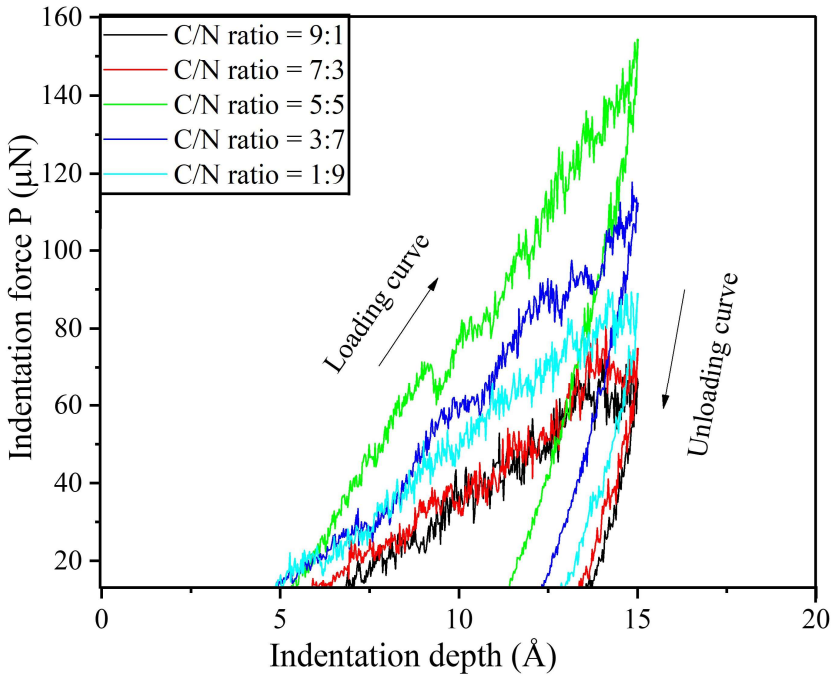

Figure 6. Graph showing the process of testing the effect of the C/N atomic ratio on the hardness of the TiAlCN film.

These structural differences directly govern the hardness response of the coating. TiN- and TiC-based nanocrystalline phases exhibit high intrinsic hardness caused by strong covalent–ionic bonding and high resistance to plastic deformation, whereas the amorphous carbon regions possess lower load-bearing capability [2,9,28]. Consequently, coatings with an excessive carbon content show reduced hardness, whereas nitrogen-rich coatings exhibit only moderate hardness. The optimal hardness observed at C/N ≈ 5:5 arises from the synergistic effect between the hard nanocrystalline phases and a refined nanocomposite microstructure, which effectively impedes deformation and enhances the overall mechanical performance of the coating [9,19], as shown in Figure 7.

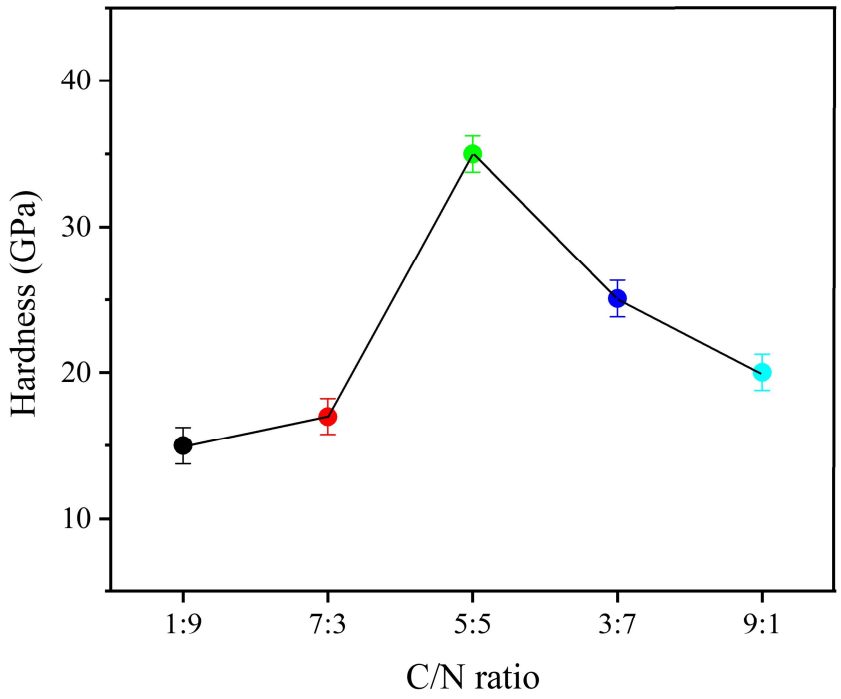

Figure 7. Graph illustrating the effect of the C/N atomic ratio on the hardness of the TiAlCN film.

3.2. Surface roughness

Using OVITO software to visualize the surface morphology of the samples under varying Ti/Al atomic ratios, we obtained the images shown in Figure 8.

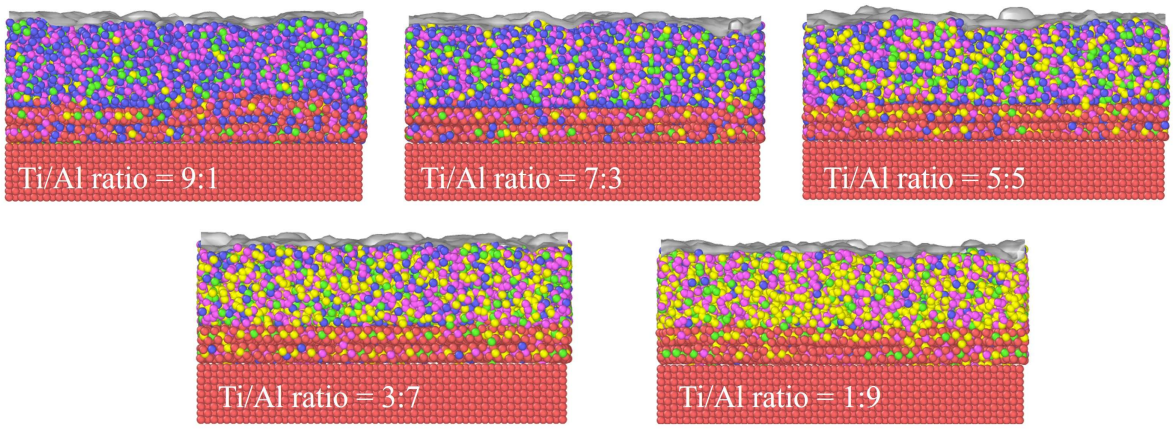

Figure 8. Effect of the Ti/Al atomic ratio on the surface of the TiAlCN film.

From Figure 9, it can be observed that when the Ti/Al ratio decreases from 9:1 to 7:3, the surface roughness slightly decreases. This may be attributed to the formation of finer AlN or TiAlN phases as the Al content increases. When the Ti/Al ratio is further reduced from 7:3 to 5:5, the roughness remains at the lowest stable level, which could represent the optimal condition for forming a coating with

smaller and smoother grain sizes. As the Ti/Al ratio continues to decrease from 3:7 to 1:9, the roughness begins to increase again, particularly at the 1:9 ratio. This may be due to the formation of hexagonal AlN (h-AlN) phases with coarser structures, where changes in the crystallization mechanism increase grain size. The occurrence of defects or uneven adhesion processes may also contribute to this effect. However, the variation in roughness is not significant because the atomic radii of Ti and Al are relatively similar.

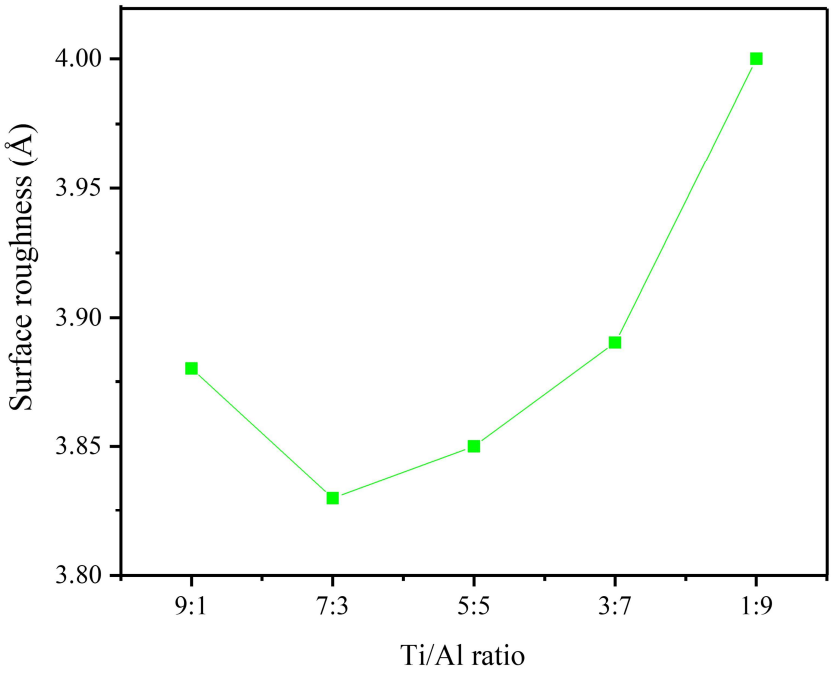

Figure 9. Graph of the influence of the Ti/Al atomic ratio on the roughness of the TiAlCN film.

As seen in Figure 10, as the C/N ratio decreased from 9:1 to 5:5, the surface roughness gradually declined. This behavior can be attributed to the formation of TiC or amorphous carbon (a-C) phases, which contribute to surface smoothing. At the 5:5 ratio, the roughness reached its minimum value, which may represent the optimal composition for achieving a uniform coating with fine crystalline grains. When the C/N ratio was further reduced from 3:7 to 1:9, the roughness slightly increased again, as shown in Figure 11. This can be explained by the formation of coarser carbon-containing phases, accompanied by changes in the coating's crystallization process and an uneven phase distribution.

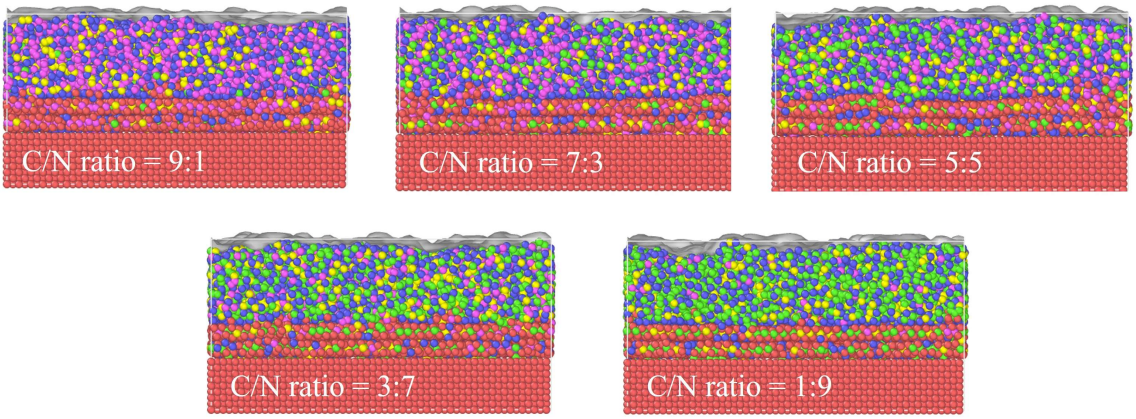

Figure 10. Effect of the C/N atomic ratio on the surface of the TiAlCN film.

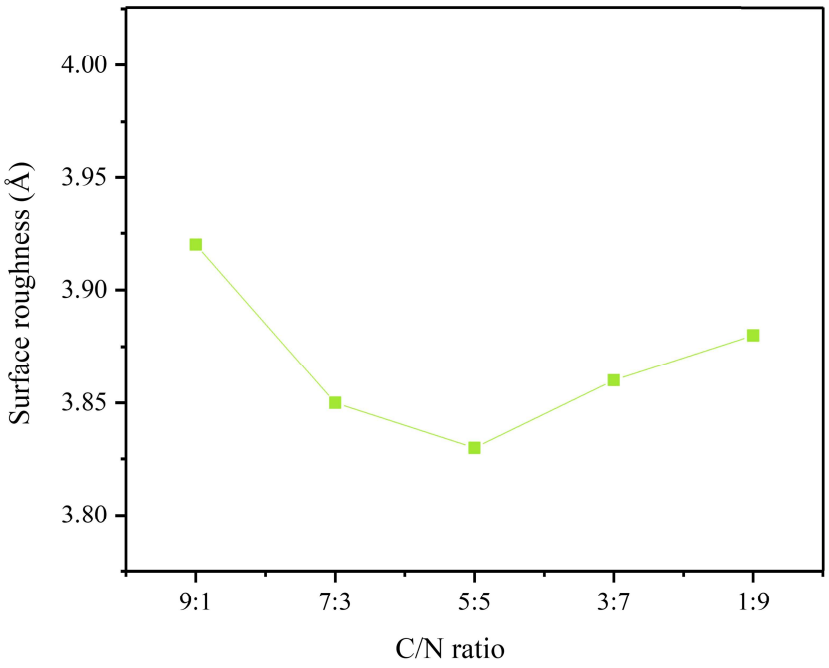

Figure 11. Graph of the influence of the C/N atomic ratio on the roughness of the TiAlCN film.

3.3. Coefficient of friction

The coefficient of friction of the TiAlCN coating in this study was determined through atomic-scale scratch testing simulations. A virtual spherical indenter with a radius of R = 10 Å was used. The indenter was first pressed perpendicularly into the coating surface to a penetration depth of 15 Å and then moved along the *Ox* direction over a sliding distance of 65 Å, as shown in Figure 12.

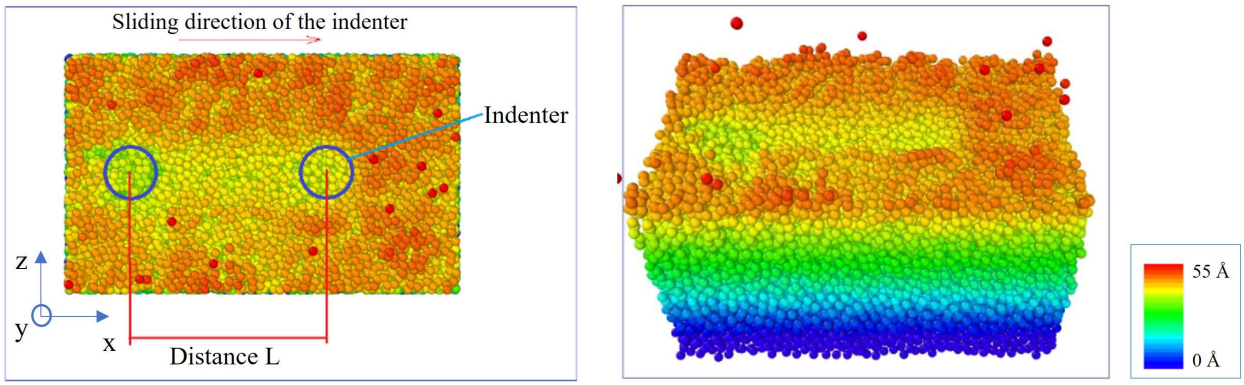

Figure 12. Schematic diagram of the test of the TiAlCN film's friction coefficient.

From Figure 13, we can see that the Ti/Al atomic ratio primarily affects the microstructure and hardness of the TiAlCN coating, indirectly influencing the friction coefficient through phase stability and surface morphology. A higher Ti content (lower Al) promotes the formation of hard TiN phases, increasing hardness but potentially raising friction because of the rougher surface and reduced oxidation resistance. A higher Al content (lower Ti) increases the AlN phases, enhancing thermal stability but possibly reducing hardness and leading to phase separation, which can increase friction under high-load conditions. Overall, the Ti/Al ratio has a moderate effect on friction, with an optimal ratio (e.g., Ti/Al ≈ 7:3) helping to minimize friction by balancing the phases. The coefficient of friction resulting from the calculation is given in Table 3.

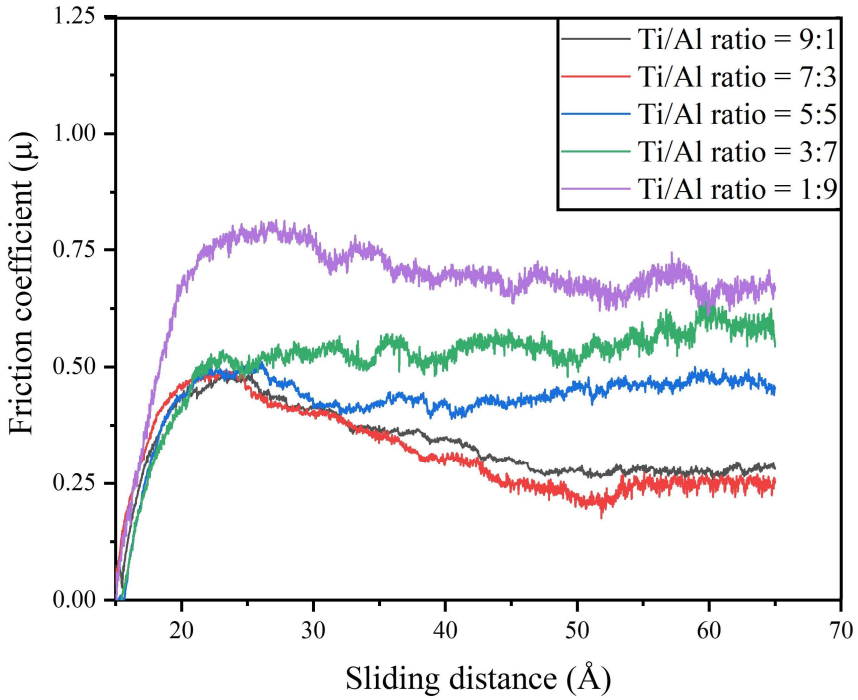

Figure 13. Graph of the influence of the Ti/Al atomic ratio on the friction coefficient of the TiAlCN film.

Table 3. Coefficient of friction of the TiAlCN film when changing the Ti/Al atomic ratio.

Ti/Al ratio	Coefficient of friction
9:1	0.27
7:3	0.25
5:5	0.43
3:7	0.56
1:9	0.64

In Figure 14, the C/N ratio has a stronger influence on the friction coefficient. Increasing the carbon content reduces friction by forming carbon-rich lubricating phases (sp^3-hybridized DLC structures), lowering the coefficient from ≈0.65 to ≈0.38. This occurs because the addition of carbon creates low-shear interfaces. However, an excessive carbon content can increase surface roughness and defects, slightly raising friction. An optimal C/N ratio (e.g., ≈5:5) yields the lowest friction coefficient of ≈0.38, as shown in Table 4 The C/N ratio impacts the friction coefficient more significantly because the addition of carbon directly produces low-friction phases, whereas the Ti/Al ratio primarily affects hardness and indirectly influences the tribological properties.

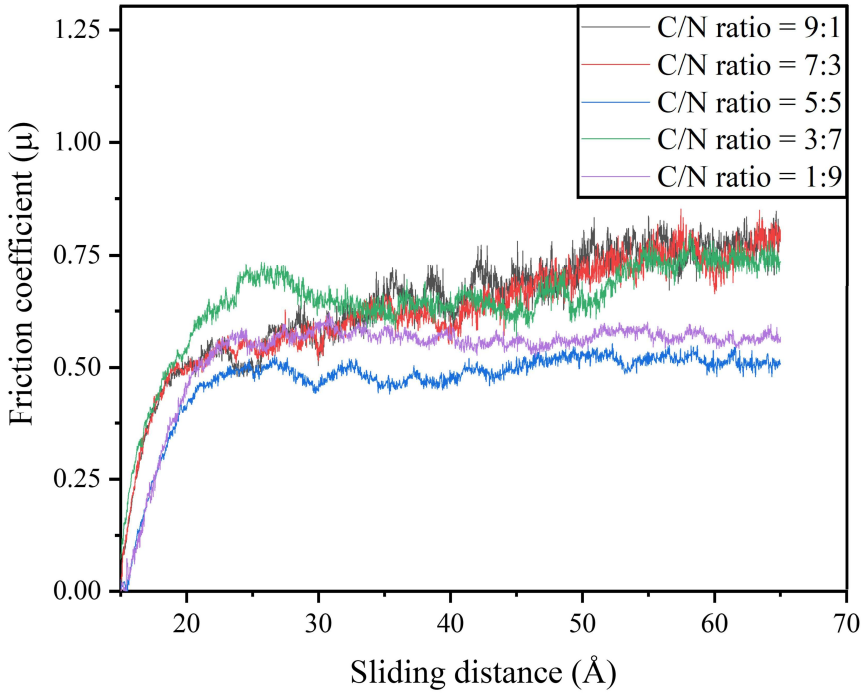

Figure 14. Graph of the influence of the C/N atomic ratio on the friction coefficient of the TiAlCN film.

Table 4. Coefficient of friction of the TiAlCN film when changing the atomic ratio of C/N.

C/N ratio	Coefficient of friction
9:1	0.65
7:3	0.63
5:5	0.38
3:7	0.50
1:9	0.62

4. Conclusions

The good agreement between the simulation results and experimental data reported in the literature further confirms the reliability of the proposed MD model.

This study systematically investigated the effects of Ti/Al and C/N atomic ratios on the mechanical and tribological properties of TiAlCN coatings using MD simulations. The results indicate that increasing the Ti/Al ratio leads to a more uniform crystal structure, resulting in improved hardness and wear resistance. In contrast, the C/N ratio plays a dominant role in governing the friction behavior, where higher carbon content promotes the formation of a-C and CNx phases, which act as solid lubricants and effectively reduce friction within an optimal composition range. Good agreement between the simulation and experimental results confirms the reliability of the proposed model.

Overall, the findings demonstrate that the C/N ratio has a stronger influence on hardness, while variations in Al content tend to affect surface roughness more significantly. These insights provide a useful guideline for tailoring TiAlCN coatings with a balanced combination of high hardness and low friction for cutting and wear-resistant applications. Future work will focus on extending the composition range, incorporating temperature effects, and exploring multilayer architectures to further enhance coatings' performance under practical service conditions.

Use of AI tools declaration

The authors declare they have not used Artificial Intelligence (AI) tools in the creation of this article.

Author contributions

Duc Cuong Pham: review & editing; Duc Luan Nguyen: writing–original draft, visualization, validation, supervision, software.

Conflict of interest

The authors declare no conflict of interest.

References

1. Anders A (2008) *Cathodic Arcs: From Fractal Spots to Energetic Condensation*, NY: Springer New York. https://doi.org/10.1007/978-0-387-79108-1

2. Mayrhofer PH, Mitterer C, Hultman L, et al. (2006) Microstructural design of hard coatings. *Prog Mater Sci* 51: 1032–1114. https://doi.org/10.1016/j.pmatsci.2006.02.002
3. PalDey S, Deevi SC (2003) Single layer and multilayer wear resistant coatings of (Ti,Al)N: A review. *Mater Sci Eng A* 342: 58–79. https://doi.org/10.1016/s0921-5093(02)00259-9
4. Sousa VFC, Da Silva FJG, Pinto GF, et al. (2021) Characteristics and wear mechanisms of TiAlN-based coatings for machining applications: A comprehensive review. *Metals* 11: 260. https://doi.org/10.3390/met11020260
5. Cheng YC, Li JX, Liu F, et al. (2025) The mechanical performance enhancement of the CrN/TiAlCN coating on GCr15 bearing steel by controlling the nitrogen flow rate in the transition layer. *Coatings* 15: 254. https://doi.org/10.3390/coatings15030254
6. Lei Z, Zhu X, Li Y, et al. (2018) Characterization and tribological behavior of TiAlN/TiAlCN multilayer coatings. *J Tribol* 140: 051301. https://doi.org/10.1115/1.4039723
7. Chen L, Xu YX, Du Y, et al. (2015) Effect of bilayer period on structure, mechanical and thermal properties of TiAlN/AlTiN multilayer coatings. *Thin Solid Films* 592: 207–214. https://doi.org/10.1016/J.TSF.2015.09.029
8. Naghashzadeh AR, Shafyei A, Sourani F (2022) Nanoindentation and tribological behavior of TiN-TiCN-TiAlN multilayer coatings on AISI D3 tool steel. *J Mater Eng Perform* 31: 4335–4342. https://doi.org/10.1007/s11665-021-06533-2
9. Musil J (2000) Hard and superhard nanocomposite coatings. *Surf Coat Technol* 125: 322–330. https://doi.org/10.1016/S0257-8972(99)00586-1
10. Endrino JL, Fox-Rabinovich GS, Gey C (2006) Hard AlTiN, AlCrN PVD coatings for machining of austenitic stainless steel. *Surf Coat Technol* 200: 6840–6845. https://doi.org/10.1016/j.surfcoat.2005.10.030
11. Fox-Rabinovich GS, Yamamoto K, Veldhuis SC, et al (2005) Tribological adaptability of TiAlCrN PVD coatings under high performance dry machining conditions. *Surf Coat Technol* 200: 1804–1813. https://doi.org/10.1016/j.surfcoat.2005.08.057
12. Zhang X, Jiang J, Zeng, et al. (2009) Effect of carbon on TiAlCN coatings deposited by reactive magnetron sputtering. *Surf Coat Technol* 203: 594–597. https://doi.org/10.1016/j.surfcoat.2008.06.175
13. Zhou B, Wang Y, Liu Z, et al (2023) Effect of modulation ratio on microstructure and tribological properties of TiAlN/TiAlCN multilayer coatings prepared by multi-excitation source plasma. *Vacuum* 211: 111917. https://doi.org/10.1016/j.vacuum.2023.111917
14. Yan N, Zhu Z, Cheng Y, et al. (2024) Preparation and performance of a Cr/CrN/TiAlCN composite coating on a GCr15 bearing steel surface. *Coatings* 14: 782. https://doi.org/10.3390/coatings14070782
15. Walunj G, Choudhari A, Digole S, et al. (2024) Microstructure, mechanical, and tribological behaviour of spark plasma sintered TiN, TiC, TiCN, TaN, and NbN ceramic coatings on titanium substrate. *Metals* 14: 1437. https://doi.org/10.3390/met14121437
16. Kumar N, Krishnan R, Dinesh Kumar D, et al. (2011) Tribological properties of nanostructured TiC coatings deposited on steel and silicon substrates using pulse laser deposition technique. *Tribol-Mater Surf Interfaces* 5: 1–9. https://doi.org/10.1179/1751584X10Y.0000000006
17. Rashidi M, Tamizifar M, Boutorabi SMA (2020) Characteristics of TiAlCN ceramic coatings prepared via pulsed-DC PACVD, part I: Influence of precursors' ratio. *Ceram Int* 46: 1269–1280. https://doi.org/10.1016/j.ceramint.2019.06.303

18. Moritz Y, Kainz C, Tkadletz M, et al. (2021) Microstructure and mechanical properties of arc evaporated Ti(Al,Si)N coatings. *Surf Coat Technol* 421: 127461. https://doi.org/10.1016/j.surfcoat.2021.127461
19. Chen SN, Zhao YM, Zhang YF, et al. (2021) Influence of carbon content on the structure and tribocorrosion properties of TiAlCN/TiAlN/TiAl multilayer composite coatings. *Surf Coat Technol* 411: 126886. https://doi.org/10.1016/j.surfcoat.2021.126886
20. Baskes MI (1992) Modified embedded-atom potentials for cubic materials and impurities. *Phys Rev B* 46: 2727–2742. https://doi.org/10.1103/PhysRevB.46.2727
21. Tersoff J (1988) Empirical interatomic potential for carbon, with applications to amorphous carbon. *Phys Rev Lett* 61: 2879–2882. https://doi.org/10.1103/PhysRevLett.61.2879
22. Vashishta P, Kalia RK, Rino JP, et al. (1990) Interaction potential for SiO_2: A molecular-dynamics study of structural correlations. *Phys Rev B* 41: 12197–12209. https://doi.org/10.1103/PhysRevB.41.12197
23. Thompson AP, Aktulga HM, Berger R, et al. (2022) LAMMPS–A flexible simulation tool for particle-based materials modeling at the atomic, meso, and continuum scales. *Comput Phys Commun* 271: 108171. https://doi.org/10.1016/j.cpc.2021.108171
24. Brown IG (1998) Cathodic arc deposition of films. *Annu Rev Mater Sci* 28: 243–269. https://doi.org/10.1146/annurev.matsci.28.1.243
25. Oliver WC, Pharr GM (1992) An improved technique for determining hardness and elastic modulus using load and displacement sensing indentation experiments. *J Mater Res* 7: 1564–1583. https://doi.org/10.1557/JMR.1992.1564
26. Persson BNJ (2000) *Sliding Friction: Physical Principles and Applications*, Heidelberg: Springer Berlin. https://doi.org/10.1007/978-3-662-04283-0
27. Müser MH, Urbakh M, Robbins MO (2003) Statistical mechanics of static and low-velocity kinetic friction, In: Prigogine I, Rice SA, *Advances in Chemical Physics*, New York: Wiley, 187–272. https://doi.org/10.1002/0471428019.ch5
28. Fischer-Cripps AC (2011) *Nanoindentation*, 3Eds., NY: Springer New York. https://doi.org/10.1007/978-1-4419-9872-9
29. Dobierzewska-Mozrzymas E, Rysiakiewicz-Pasek E, Biegański P, et al. (2008) Application of the optical method for determining of the RMS roughness of porous glass surfaces. *J Non Cryst Solids* 354: 3241–3245. https://doi.org/10.1016/j.jnoncrysol.2008.02.013

AIMS Press